Pharm Res (2011) 28:647–661
DOI 10.1007/s11095-010-0319-z

RESEARCH PAPER

A Smart Interface for Reliable Intradermal Injection and Infusion of High and Low Viscosity Solutions

Michael Vosseler • Michael Jugl • Roland Zengerle

Received: 28 July 2010 / Accepted: 1 November 2010 / Published online: 23 November 2010

ABSTRACT

Purpose We present a smart intradermal interface suitable for skin-attached drug delivery devices. Our solution enables injections or infusions that are less invasive compared to subcutaneous injections and are leakage-free at the location of penetration.

Methods The intradermal interface is based on a 31-gauge cannula embedded in a slider, movable relative to a carrier plate that can easily be fixed onto the skin. By simply pushing the slider, the cannula is inserted into the dermis.

Results We performed injections and infusions with stained water and polyethylene glycol (PEG) solution in *ex vivo* pig skin. The sizes of coloured spots in the skin range from 3.5 mm^2 to 15.4 mm^2 for stained water depending on the infused volume. Infusing stained PEG solution resulted in stained tissue areas about one order of magnitude larger. One of three investigated leakage modes is unacceptable but can be reliably avoided by proper site selection. At low flow rates and at the beginning of an infusion an initial back pressure overshoot was identified. This effect was identified as the limiting parameter for the design of small programmable or intelligent devices based on micro actuators.

Conclusions With the proposed easy-to-use interface, intradermal injections and infusions can be performed reliably. Therefore, it is supposed to be an ideal and clinically relevant solution for self-administration of parenteral drugs in home care applications.

KEY WORDS drug delivery · infusion · injection · intradermal · microneedle

M. Vosseler (✉) · M. Jugl · R. Zengerle
HSG-IMIT
Wilhelm-Schickard-Str. 10
78052, Villingen-Schwenningen, Germany
e-mail: michael.vosseler@hsg-imit.de

R. Zengerle
Laboratory for MEMS Applications
Department of Microsystems Engineering—IMTEK
University of Freiburg
Georges-Koehler Allee 106
79110, Freiburg, Germany

INTRODUCTION

For almost one century intradermal injections were performed nearly exclusively with the Mantoux method (1–3). This method describes the use of a 25- or 27-gauge hypodermic needle (outer diameter: 0.51 mm or 0.41 mm respectively) inserted almost parallel to the skin surface. After proper injection of 0.1 ml–0.2 ml of fluid a raised papule (wheal) indicates a successful intradermal injection. The Mantoux method is difficult to perform and requires trained and experienced personnel. For that reason intradermal injections have mainly been used in flu epidemics with a shortage of vaccines. Nowadays, intradermal drug delivery is considered as a potential route for the delivery of parenteral drugs like insulin and therapeutic antibodies. It is less invasive compared to subcutaneous injections and infusions and offers the additional advantage of accelerated pharmacokinetics (4). To utilise these benefits there is a need for a reliable, easy-to-use method to accomplish intradermal injections and infusions in a self-administrable manner.

In general, the skin is getting more and more attention as a potential route for *systemic drug delivery* since the market approval of the first transdermal therapeutic system (TTS), in 1979, which uses drug-loaded patches to diffuse drug into the body due to the concentration gradient. Drug is absorbed by the bloodstream in the capillaries of the papillary dermis, which is located approximately 0.2 mm

below the skin surface. In contrast, vaccination is an example of *local drug delivery*, which targets the numerous Langerhans cells in the epidermis, the outer skin layer above the papillary dermis. These cells capture, take up and process antigens.

The benefits of the first generation TTS is the circumvention of first-pass metabolism, continuous release of the drug over longer periods of time, non-invasiveness and self-administration capability. All these benefits result in better patient compliance. However, the current available TTS are limited to non-ionic, lipophilic drugs with a molecular weight below 500 Da. Hydrophilic, ionic and especially macromolecular drugs can not be delivered with this technology. The reason for this limitation is the stratum corneum, the outer part of the epidermis, which consists of dead keratinocytes in a lipid matrix. The thickness of this layer is about 0.01 mm–0.02 mm. It blocks most of the molecules of therapeutic interest. With an easy-to-use and reliable method for intradermal infusions and injections this limit is no longer relevant, so, for the sake of minimal invasiveness, the benefits of TTS can be applied to almost any drug.

Circumventing the stratum corneum by intradermal infusions or injections is just one of several possible approaches. An alternative state-of-the-art method to increase skin permeation is the use of chemical penetration enhancers. Apart form that, other methods and technologies currently under investigation include heat, skin abrasion, thermal ablation, electroporation, iontophoresis, ultrasound and solid as well as hollow microneedles (5–7).

Hollow microneedles can be made of various materials, such as silicon (8–10), glass (11), polymer (12,13) or metal (2,14), by a wide range of different fabrication technologies. Typical dimensions of an individual hollow microneedle are up to 0.8 mm in length, an outer diameter of up to 0.3 mm and an inner diameter up to 0.15 mm. For microneedle arrays with short microneedles a special application procedure may be necessary (15). The outer diameter is just a rough approximation because the cross-section of a hollow microneedle is not necessarily circular (8). Also, steel cannulas with a size of 30 gauge (outer diameter 0.31 mm) or higher are considered microneedles (16). Most technologies allow arranging several microneedles into a microneedle array. Arrays made of three to four microneedles are regarded to be sufficient in order to distribute the drug to a larger area within the skin and are currently in clinical studies (3,17). Microneedles allow lower microbial penetration than a 21-gauge hypodermic needle (18).

The most important prerequisite for clinical acceptance of hollow microneedles is the delivery of a consistent amount of drug to the intradermal layer without any leakage. Many microneedle designs discussed in the literature did not comment on this very important issue. However, recent studies examining this topic (2,3,19) reveal that leakage can be an issue. Microneedles with round cross-section seem to be superior to microneedles with other cross-sections.

Hollow microneedles enable delivery of drugs in a continuous fashion or, alternatively, in intervals that are defined by time, sensor signals or user input if those needles are integrated in a suitable drug delivery system (20,21). Precise time-controlled (delayed or pulsatile) drug delivery, for example, is necessary for chronopharmaceutical applications (22).

For selection of an adequate actuation mechanism of the extracorporal drug delivery device (23) it is necessary to identify the back pressure during an intradermal injection or infusion via a microneedle array. In a previous study, the flow rate as a function of applied pressure was studied (11). The single microneedle was inserted perpendicular to the skin surface. During this process, the skin tissue got compressed. Partial retraction of the needle reduced the compression in the skin. According to the presented data, flow rate is a function of insertion depth, retraction distance and applied pressure. As a consequence, it is stated that drug delivery devices to be combined with microneedles should be based on a flow-controlled boundary condition instead of a simple pressure control.

In this paper, we present a new transdermal interface consisting of a microneedle as well as a defined mechanism for its insertion. We characterize this transdermal interface by using two classes of liquids: a low viscosity solution based on stained water and a high viscosity solution based on stained polyethylene glycol (PEG). For the infusion experiments, we used a flow-controlled syringe pump. The injections were done by manual operation of a syringe. We investigate the vertical penetration depths depending on penetration parameters, the leak tightness, the distribution of the staining within the tissue as well as the transient back pressures that occur during infusions or injections.

MATERIALS AND METHODS

Pig Skin

Excised pig skin was used in the experiments because of its easy availability. It shows similarity to human skin in terms of morphology and permeability characteristics (24). However, there is a higher density of collagen and other fibre bundles in the reticular (lower part of the) dermis (2) that results in reduced skin elasticity and increased resistance to skin deformability.

Non-blanched pig ears were obtained from a local slaughterhouse. The ears were cleaned with fresh water. Skin specimens were prepared by removing the skin from

the backside of the ear with a scalpel and punching discs with 30 mm diameter. The average weight of the skin specimens is 1.36 g±0.34 g. Ears and skin specimens were stored in a freezer at −18°C until needed. The average thickness, measured in the frozen state, is 2.51 mm± 0.45 mm, resulting in a specimen volume of 1.77 ml± 0.32 ml. No ear and no skin specimen were stored longer than 3 months. The skin was not shaved.

Solutions for Injection and Infusion

Infusion/injection experiments were performed with water (vehicle)-based solution containing 0.90 wt. % NaCl and 0.02 wt. % gentian violet (solute) for staining. A second solution based on PEG 200 (vehicle) with 0.02 wt. % gentian violet (solute) was prepared. All chemicals were obtained form Merck KGaA, Darmstadt, Germany.

PEG 200 is a Newtonian fluid.[1] It is completely miscible with water and octanol (25), is chemically inert and has low toxicity. Its viscosity was determined to be 55 mPas. PEG 200 is a low molecular weight (200 g/mol) species with diol characteristics. It has a high vascular permeability compared to high molecular weight PEG such as PEG 30.000 (26).

Gentian violet is positively charged in neutral aqueous solutions, has a molecular weight of 408 g/mol and has an octanol water partition coefficient of log P=0.51. Gentian violet can bind to proteins, e.g. Human Serum Albumin (27), and human cells, e.g. epidermal cells (28). Its maximum solubility is 1.1 g in 100 ml of water and 13.9 g in 100 ml ethanol. Its solubility in PEG 200 is good due to the diol characteristics of the low molecular weight species. Therefore, gentian violet in PEG is less staining than gentian violet in water if it is used, for example, in the eradication of bacteria-afflicted skin (29).

Laboratory Penetration Setup

Penetration of a cannula almost parallel to the skin surface without stretching the skin generates wrinkles. In order to reduce those wrinkles, together with all the complex failure mechanisms affiliated with them, we implemented a wrinkle-free penetration mechanism as follows. By simply pushing a slider on a carrier plate, the cannula is inserted by a well-defined displacement x (Fig. 1) at a well-defined angle of 10° into the skin. By releasing the slider, the cannula is pushed back automatically by a second well-defined displacement (x-y) in order to relax the skin. Finally, that mechanism results in a well-defined lateral penetration length w and vertical penetration depth z_w of the tip of the cannula in the skin.

The laboratory setup is shown in Figs. 1 and 2. It consists of a vertically moveable carrier plate (a) made of clear PMMA. It can be locked several centimetres above the base plate (b). A replaceable cannula (c) is fixed to a slider (d) which can move on two shafts (e) between the stop bar (f) and the carrier plate (a). In its initial state, the spring (g) pushes the slider (d) towards the stop bar (f). The cannula is mounted into the slider (d) in such a way that the distance of its tip to the skin surface is zero when no forces are applied. In that position the distance of the tip to the bottom of the carrier plate (a) equals z_1, which corresponds to the thickness of the stack of double-sided adhesive tape (i) and medical tape (j) (Hansaplast classic tape by Beiersdorf AG, Hamburg, Germany). The sticky side of the medical tape is directed downwards to fix the pig skin. The stack of tapes has a width of 25 mm with a circular hole of 4 mm radius around the cannula. This hole forms a bulge-defining cavity. The skin deforms and can fill this cavity if forces are applied.

The maximum displacement x of the cannula during insertion is defined by the distance between the stop bar (f) and the carrier plate (a). The theoretical maximum vertical penetration depth of the cannula tip in the tissue during the penetration is z_3, assuming that the skin bulges into the bulge-defining cavity and is limited by direct contact with the bottom of the carrier plate.

By releasing the slider, the cannula is pushed back due to the spring (g). The final vertical penetration depth, z_2, of the cannula tip during the infusion experiments is defined by an exchangeable spacer (h) that is placed in between the slider (d) and the stop bar (f) before releasing the slider. z_2 can be calculated to be $z_1+y*\sin 10°$ (Fig. 1).

By adjusting the stop bar (f), it is possible to vary the maximum displacement, x, of the cannula (d). The insertion parameters of all infusion/injection experiments in this paper are summarised in Table I. Infusion experiments were performed with insertion parameter sets 3/1, 4/2, 5/3. x/y denotes the displacement sets, x and y, as depicted in Fig. 1 and tabulated in Table I.

For all experiments 31-gauge stainless steel cannulas with an outer diameter of 0.26 mm, an inner diameter of 0.13 mm (min. 0.11 mm, max. 0.15 mm), a length of 30 mm and a bevelled tip (14°) were used. The length of the tip is 1.0 mm. The cannula was always mounted bevelled side up. Its fluidic resistivity was theoretically calculated according to Hagen-Poiseuille to 1.2 kPa h/ml. Hydrodynamic effects caused by the orifice of the cannula are neglected due the high aspect ratio (length per diameter) of 115. The experimental verification resulted in a fluidic resistivity of 0.9 kPah/ml±0.1 kPah/ml corresponding to an effective inner diameter of 0.14 mm.

[1] Overview Brochure Carbowax PEG, The Dow Chemical Company, Midland, Michigan, USA

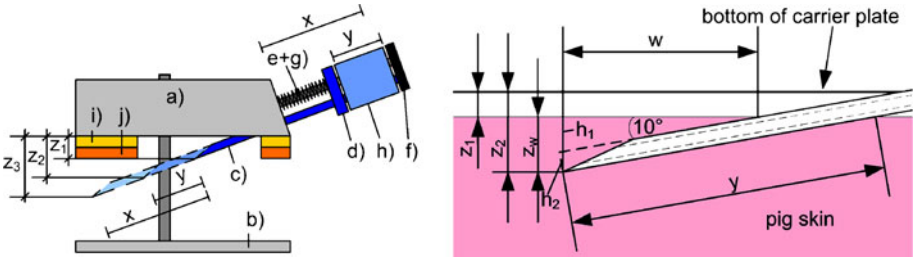

Fig. 1 Left: Sketch of the laboratory setup for well-controlled insertion of a cannula into a skin specimen with a small defined angle of 10°. Right: Cannula at infusion position. Details explained in the text.

Fluidic Setup

The fluidic setup consists of the cannula, the tubing, a flow sensor, a pressure sensor and a syringe made of glass. To keep the fluidic capacity of the whole setup as small as possible, stiff FEP (fluorinated ethylene-propylene) tubings were used. FEP is a transparent material, so bubble-free priming can be controlled easily. The fluidic resistance of the tubing (outer diameter: 1.6 mm, inner diameter: 0.8 mm) per centimetre is four orders of magnitude smaller compared to the fluidic resistance of the cannula. Therefore, it can be neglected. Glass syringes (10 ml volume for infusion experiments, 0.1 ml and 0.5 ml volume for injection experiments) were used because of their negligible fluidic capacity. A laboratory syringe pump (MDSP3f by MMT Micro Mechatronic Technologies GmbH, Siegen, Germany) was used to enable flow-controlled liquid delivery in the infusion experiments. The glass syringe was driven manually in the injection experiments. A metronome was used for the timing of this manual injection process. The flow rate in the tubing was monitored with a flow sensor (Liqui-Flow by Bronkhorst, Ruurlo, Netherlands) with a maximum measurement range of 5 ml/h. Depending on the expected back pressure, one out four pressure sensors (two different sensors of type EPX by Entran Sensors, Potterspury, United Kingdom; PDCR 200 by GE Sensing, Billerica, USA and CTE8000 by SensorTechnics, Puchheim, Germany) was integrated in the setup to measure the back pressure generated by the needle and the tissue. The measurement ranges of the sensors are 100 kPa, 350 kPa, 600 kPa, and 1,000 kPa, respectively. The selected sensor was mounted downstream (after the flow sensor), and the pressure offset was levelled to zero before the infusion took place. This way, the pressure difference along the needle plus the tissue was recorded.

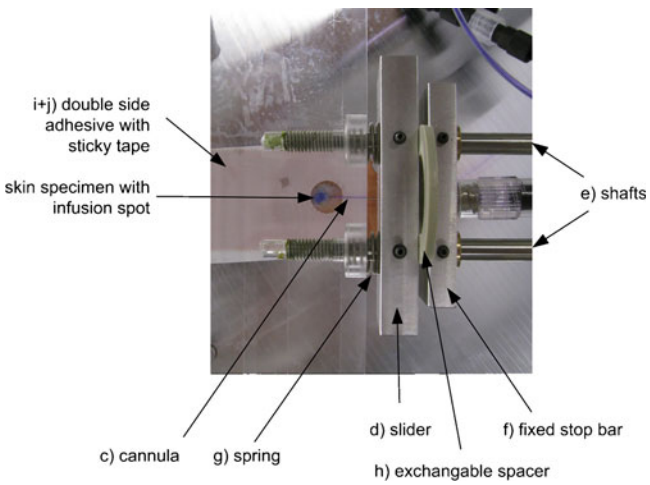

Fig. 2 Close-up photo of the laboratory setup for well-controllable insertion of a cannula into a skin specimen.

Based on the above statements the following fluidic model for the infusion/injection experiments is assumed (Fig. 3). It is a parallel circuit of a fluidic capacity and a fluidic resistor. The experimental setup is modelled as a capacity (C_{setup}), neglecting its fluidic resistivity. The cannula is modelled as a constant resistor ($R_{cannula}$). Its capacity is neglected due to the high stiffness of metal tubing. The tissue is also modelled as a resistor (R_{tissue}). This assumption is checked in the results section. The flow, q, generated by the syringe pump or by pressing the syringe generates the pressure drop, p.

Injection and Infusion Experiments

To perform an infusion or injection experiment, the carrier plate was locked well above the base plate. A piece of artificial skin (skin suture trainer by 3B Scientific, Hamburg, Germany) was wrapped in cling wrap and placed on the base plate. A pig skin specimen was placed on top of it, and the carrier plate was

Table 1 Sets of Insertion Parameters of the Injection and Infusion Experiments

x / mm	y / mm	z_1 / mm	z_2 / mm	z_3 / mm
3	1	0.45	0.62	0.97
4	2	0.45	0.80	1.14
5	3	0.45	0.97	1.32

x is the maximum displacement of the cannula (c) in Fig. 1. y is the final displacement of the cannula for infusions / injections. z_1 is the depth of the bulge defining cavity and defined by the thickness of the stack of double side adhesive (i) and tape (j). z_2 and z_3 are the vertical distance of the cannula tip to the bottom of the carrier plate. They are defined by the displacements y and x, respectively.

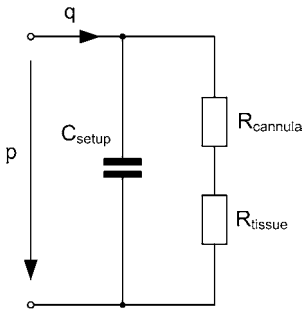

Fig. 3 Assumed model for the intradermal infusion / injection experiments.

lowered down until it got in contact with the skin. Immediately, the skin specimen stuck to the sticky tape at the bottom of the carrier plate. The cannula was inserted in the skin according to the method described before.

After the insertion of the cannula and before starting the experiments, the carrier plate with the skin specimen attached to it was lifted again and locked in its upper position. This way, there was no mechanical pressure applied on the skin during the infusion/injection experiments.

Infusion experiments were performed with all three sets of insertion parameters listed in Table I. A volume of 0.20 ml and 1.00 ml was infused in 2 h at flow rates of 0.10 ml/h and 0.50 ml/h, respectively. Experiments with the high viscosity PEG solution were done with both flow rates but only with the insertion parameter set $x=4$ mm and $y=2$ mm.

Injection experiments were always performed with insertion parameters $x=4$ mm and $y=2$ mm. Only the water-based solution was used for the injection experiments. Two different sets of injection experiments were performed. In the first set, 0.10 ml of volume was injected in 10 s (average flow rate: 36 ml/h). In the second set, a volume of 0.50 ml was injected in 10 s (average flow rate: 180 ml/h).

For an infusion/injection experiment with a fixed set of insertion parameters at least nine skin specimens were prepared from skin of three different pigs. At least three skin specimens came from the same individual pig, respectively. All together, 92 experiments were performed: 56 infusion experiments and 18 injection experiments with the water-based solutions as well as 18 infusion experiments with the PEG-based solutions.

To estimate the diffusion of the dye in the skin, 0.50 ml of aqueous solution and 0.10 ml of PEG solution were injected in skin specimens. The spot area was measured after injection and 2 h later.

Leakage was detected and quantified by the following method. If any leakage was observed, a droplet of infusion/injection solution with a volume of 5 µl was placed on top of the skin with a microliter syringe and a cannula. The stained area of the leakage was compared to the stained area of the 5 µl droplet. In this way, it was possible to estimate leakage to be below or above 5 µl.

The clear PMMA material of the carrier plate enabled taking photos of the skin specimen and the cannula (c) by placing it under a microscope with a camera attached to it. Photographs of the cannula (c) were taken in its infusion/injection position with and without skin. Comparing the two pictures, it was possible to experimentally determine the lateral penetration length w of the cannula. After removing the cannula, photographs of the infusion spot and its cross-section were taken with a calibrated microscope/camera combination. The flow sensor and pressure sensor data were recorded during infusion with a sample rate of 10 Hz.

RESULTS AND DISCUSSION

Penetration Results

When the carrier plate (a) was lowered onto the skin specimen (k) (Figs. 1 and 4), resting on the artificial skin (l), due to the weight of the carrier plate (≈500 g), the skin bulged into the bulge-defining cavity, defined by the stack of double-sided adhesive tape (i) and medical tape (j). A notch (Fig. 4) formed around the cannula (c), which made it easy to penetrate the skin.

The cannula insertion process is presented in Fig. 5. From the pictures, it is clear that the skin deforms prior to tip penetration, so the maximum lateral tip penetration is not as deep as theoretical calculations suggest. Although the main effect of the retraction function is to regress the skin deformations, some effective retraction of the cannula can not be excluded.

Skin deformations might be prevented if there is no gap in the medical tape. In this case, the skin infusion/injection site is no longer observable, which is probably of no concern in the final end-user device.

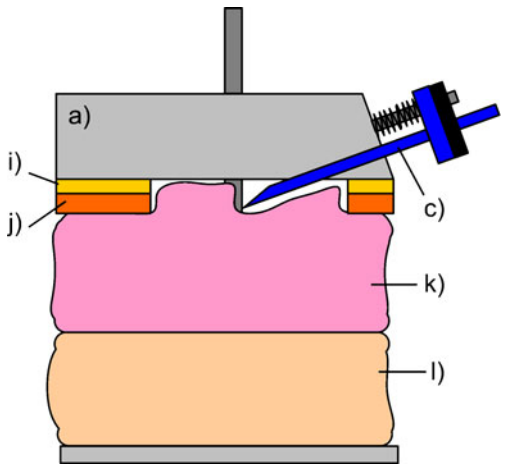

Fig. 4 Penetration setup resting on pig skin (k) and artificial skin (l). Bulging of the skin into the bulge defining cavity is shown.

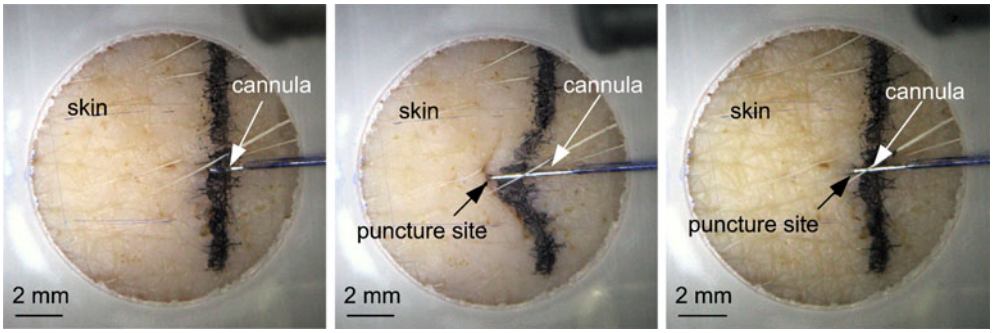

Fig. 5 Cannula insertion process. Left: The cannula tip is in its initial position on top of the skin. Middle: The cannula was pushed with the slider a distance of 4 mm at an angle of 10°. The tip punctured the skin. The deformation of the skin is indicated by the black line on the skin. Right: The slider is retracted by 2 mm. The cannula tip is in its infusion / injection position. The deformation of the skin is regressed.

The vertical penetration depth, z_w, (Fig. 1) of the cannula tip at the infusion/injection position in the skin was determined indirectly to be $h_1+h_2 = w^* \tan 10° + d/\cos 10°$ with the measured lateral penetration depth w (Fig. 1, right), the outer diameter d of the cannula (c) and a penetration angle of 10°. The vertical penetration depths vary from 0.47 mm to 0.70 mm, depending on the penetration parameters (Fig. 6) (ANOVA, $p \leq 0{,}001$). These absolute values are based on indirect measurements. However, it can be stated with very high probability that the cannula tip penetrates into the dermis. This statement is based on the assumption that the thickness of the epidermal layer is 0.20 mm. Although, there is some uncertainty in the absolute values; the relative values are supposed to be accurate.

Penetration of a cannula into the dermis is associated with stimulation of nerve endings, so the insertion process of the cannula is not pain free. Whether it is less painful compared to the insertion of a subcutaneous infusion set needs to be studied. Pain sensation during infusion/injection is a combination of pain caused by the introduction of fluid into the skin and chemical stimulation, e.g. by preservatives. Injections of 0.12 ml of fluid causes faint pain (2).

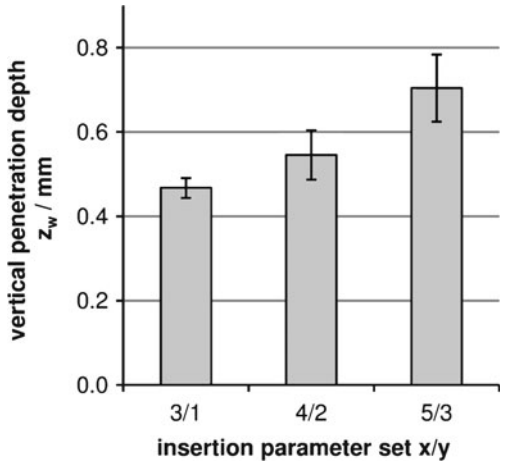

Fig. 6 Vertical penetration depths z_w of the cannula tip into the skin specimens determined by indirect measurements (see text). Each bar shows the mean and the standard deviation of at least 18 penetration experiments based on different skin storage conditions (fresh, cooled, frozen). At every set of insertion parameters the samples came from at least three different pigs.

Our original expectations regarding the vertical penetration depths were based on the assumption that the skin bulges completely into the bulge-defining cavity and is in direct contact with the bottom of the carrier plate when the tip of the cannula starts penetration of the skin as illustrated in Fig. 4. This would lead to an expected vertical penetration depth of z_2 as illustrated in Fig. 1. Comparing the indirect experimental results with those expectations, we found that the experimental values of vertical penetration depths were approximately 0.23 mm less than expected (Table I), which equals roughly half the depth of the bulge-defining cavity.

We were not able to identify any relevant influence between different individual skin samples or different storage methods (fresh, cooled up to 2 days, and frozen) on the vertical penetration depths. However, in one out of 92 experiments it was impossible to penetrate the skin with the cannula, and in three out of 92 experiments, two or three attempts were necessary to place the cannula successfully in the tissue. Yet, all four out of the 92 experiments that created difficulties were affiliated with skin specimens that were frozen and defrosted several times.

Leakage

A very important prerequisite for clinical acceptance of intradermal interfaces is leak tightness of the interface to allow delivery of consistent amounts of drug in a well-defined manner. In our tests, 83 out of 92 experiments were completely leakage-free. For the remaining nine cases, we identified three different leakage failure modes (Table II).

- Leakage mode 1 (occurred two times within 92 experiments): That failure mode results from hair follicles that were damaged during the insertion of the cannula. In

Table II Overview of All Experiments Done to Investigate Leakage Behaviour. Failure Modes and Failure Frequencies are Discussed in the Text.

	Infusion				Injection		# of incidences
	Water-based		PEG-based		Water-based		
	0.10 ml/h	0.50 ml/h	0.10 ml/h	0.50 ml/h	36 ml/h	180 ml/h	
No leakage	24	26	9	8	9	7	83
Failure mode 1	1	0	0	0	0	1	2
Failure mode 2	0	1	0	0	0	1	2
Failure mode 3	2	2	0	1	0	0	5
Experiments	27	29	9	9	9	9	92

that case, the stained fluid was leaking at the location of the hair follicle and could be detected on the skin surface. There was no leakage at the puncture site. That leakage mode is expected to depend on the hair follicles, density, which is quite high for skin from pig ears. We expect that this failure mode would happen less often in case of penetration of human skin. We also expect that due to proper selection of the application site the frequency of this failure mode could be reduced to an insignificant level for humans.

- Leakage mode 2 (occurred two times in 92 experiments): In that failure mode, a liquid volume of more than 5 µl could be detected on the skin surface. In all those cases, only clear liquid without staining (0.02 wt. % gentian violet, molecular weight of 408 g/mol) came out of the skin. In clinical infusion experiments it would have to be determined if in this leakage mode there is really a leakage of therapeutically relevant molecules or if only a small fraction of solvent or interstitial fluid without drug molecules is leaking. This investigation has to be done for every specific drug.

  It is important to mention that the leakage occurred at sites close to the puncture site but not at the puncture site itself. To investigate this in more detail we did injections based on the traditional manual Mantoux method (with a 31-gauge cannula). In those injections the same leakage mode occurred.

  We also investigated if this failure mode was affiliated with variations in the back pressure that occurred during the infusion. We were not able to identify any significant differences between the experiments with and without leakage. We also proofed that there is no relevant influence of the individual skin samples or storage methods.

- Leakage mode 3 (occurred five times in 92 experiments): In that failure mode, less than 5 µl of clear liquid without staining could be detected on the skin surface. As the leaking volumes are less than 2% of the delivered liquid volumes, this is regarded to be not relevant.

In conclusion, we expect that the presented smart intradermal interface enables leakage-free drug delivery when an application site with low hair density is properly selected. In the remaining leakage modes 2 and 3, only clear liquid without staining was detectable. It is very likely that this way no therapeutically relevant drug molecules are lost. Of course, this has to be finally confirmed in further experiments with humans and by using the drug of interest.

The penetration of the skin with a hollow cannula at an inclined angle enables intradermal infusion/injection with very good leak-proof properties. Another device which also demonstrated leak-proof intradermal delivery is described in (2). It consists of a single gauge-30 cannula which protrudes 1.5 mm of a specifically engineered structure. This structure was optimised to maximise the contact with the skin and minimise fluid leakage. The cannula is inserted perpendicular to the skin surface. During the injection it is necessary to keep light contact of the syringe tip in the skin's surface probably in order to realise the leak-proof properties of the specifically engineered structure. This device is definitely optimised for injection applications.

With the presented inclined penetration method and the traditional Mantoux method no special structure is necessary which maximises skin contact and minimises leakage. It is not necessary to press the structure against the skin which is prone to result with time in pain sensation (pressure to high) or leakage (pressure too low). Therefore, the proposed intradermal interface is best utilised in long-term (several minutes to days) applications.

Spot Formation

The spreading of the vehicle and solute of injected and infused solution in the skin is a combination of pressure-driven flow and diffusion with potential solute-vehicle, vehicle-skin and solute-skin interactions. The extent of diffusion was determined by measuring the spot area of injected liquid (0.50 ml of stained water and 0.10 ml of PEG solution) after injection and after 2 h. Within that

time, the spot area caused by injected stained water increased by 15%±9% (n=3), and the spot area of injected PEG solution increased by 30%±14% (n=3). The cross-sections of the spots were also measured, and the data were consistent with the surface data (see below). Spreading of the stained spot in the skin by diffusion is only a minor effect if water is used as vehicle. However, if PEG is used as vehicle, spreading of the stained spot by diffusion is substantial.

The spot formation at the surface of the skin during an experiment with insertion parameters 5/2 and a flow rate of 0.50 ml/h of stained water is presented in Fig. 7. The three pictures were taken at the beginning, after 1 h and after 2 h, respectively. The spot geometry was approximated by an ellipse. The area of the ellipse increased 62% during the second hour of the experiment. The increase is mainly caused by the pressure-driven infusion. This statement is supported by the minor extent of diffusion already determined in separate experiments.

The cross-section of skin specimens after infusion of water-based solution and PEG-based solution at a flow rate of 0.10 ml/h and insertion parameters 4/2 is presented in Fig. 8. The maximum vertical depth where gentian violet can be found seems to be limited to the dermal layer at a depth of approximately 1.5 mm if water is used as vehicle. The dashed line, following the skin surface, indicates a dome-shaped wheal which formed due to the injection of stained water. The dimensions of the wheal are larger than the dimensions of the stained spot. Obviously, the dye was separated from the water molecules. Unfortunately, the size of the wheal could not be determined because determining its circumference is very difficult.

With PEG as vehicle the maximum vertical depth where the dye can be found extends to the fatty tissue underneath the dermal layer. The dashed line, following the skin surface, is flat. The stained skin site felt harder compared to non-stained skin sites. This increase in hardness is due to the higher viscosity of PEG. Due to the fact that only stained skin sites felt harder, one can conclude that there is no or only minor separation between the dye and PEG.

For statistical analysis, the spots and the cross-sections of water-based infusions/injections were approximated by ellipses. The variations of stained tissue areas monitored from the top with delivered liquid volumes are given in Fig. 9, left for water- and PEG-based solutions. The plot shows data obtained with the insertion parameter set 4/2. The size of the stained spots caused by the water-based solutions increases linearly (R^2=0.98) from 3.5 mm^2 to 15.4 mm^2 with the delivered volume. This is a lateral increase of the stained area of approximately 440%, affiliated with a factor 10 between infused/injected volumes. The stained tissue areas monitored from the top caused by the PEG-based solutions are almost one order of magnitude larger compared to the spots caused by the water-based solutions.

We investigated if the lateral and/or vertical penetration depths of the stained areas are influenced by the insertion parameter sets. We used water-based solutions with the insertion parameter combinations 3/1, 4/2, 5/3. We found a trend that the area of the spot viewed from the top was maximum for the 4/2 insertion parameter set, but the differences were small and finally not significant (data not shown). The maximum vertical penetration depth of the stained area was determined by the minor axis of the stained cross-sectional ellipses. Data for insertion parameters 4/2 and variable infusion volumes are shown in Fig. 9, right. Even when the infused volume varies by a factor of 5, the maximum penetration depths of the stained tissue increases only from 0.75 mm to 1.18 mm, which is an increase of about 60%.

We further analyzed the lateral extension of the tissue staining from the cross-sections of the skin specimens. We used the major axis of the ellipse of the stained cross-section area as a measure for the maximum lateral extension of the tissue staining. We found the analysis based on the cross-section view of the sample to be completely consistent with the top view analysis.

Unfortunately, it is not possible to compare the size of wheals resulting from infusions with the two vehicles. The reason is lack of data for wheals obtained by infusion of aqueous solution, as already mentioned. Therefore, it is impossible to determine if the area of skin wheals depends on the vehicle.

Due to the infused/injected of stained water into the skin specimen, liquid escaped from the skin. Typically it appeared at the circumference of the skin specimen. It was transported from the infusion/injection site by the

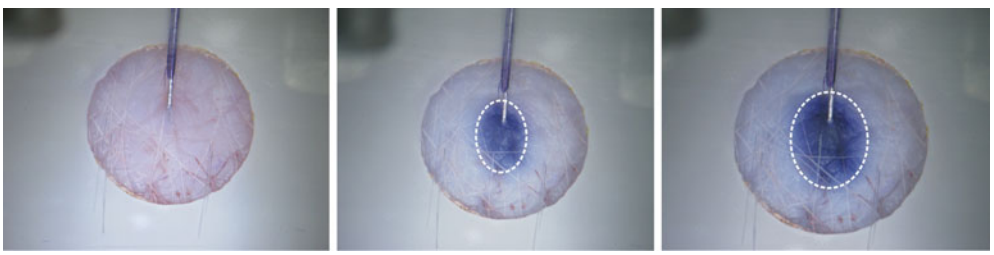

Fig. 7 Formation of a blue stained spot (top view) during a 2-h infusion of 0.02 wt. % gentian violet in 0.9% NaCl solution at 0.50 ml/h into the intradermal compartment of *ex vivo* pig skin. Left: before the infusion started, middle: after 1 h, right: after 2 h.

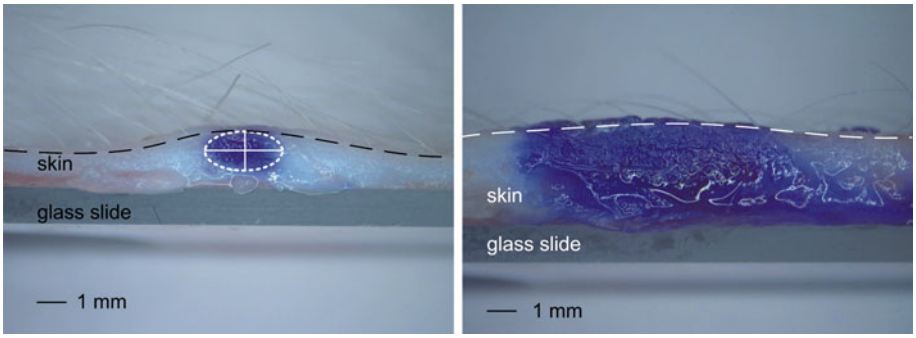

Fig. 8 Cross-sections of pig skin specimens after 2 h of infusion at a flow rate of 0.10 ml/h and insertion parameters 4/2. Left: water based solution. An ellipse with vertical (minor) and horizontal (major) axes was drawn manually to describe the cross-section of the spot as best as possible. Right: PEG-based solution. In vertical direction the skin specimen is stained completely below the tissue surface resulting in an almost perfect rectangular spot in the cross-section.

capillaries as indicated by Fig. 10. It seems that water prefers to spread in the dermis, partly forming a dome-shaped skin wheal and partly entering the capillaries instead of substantially penetrating into the hypodermis (vehicle-skin interaction). At the same time, the mainly pressure-driven distribution of gentian violet with water as vehicle is also confined to the dermis. Therefore, it is concluded, that the introduced stained water spreads in the dermis before it enters the capillaries and finally escapes the skin specimen at its circumference. The escaping liquid is almost clear. There are several reasons. As already mentioned, the water molecules separate from the dye and spread more in the dermis, so there are not only capillaries that take up water from the stained site but also capillaries that take up "filtered" water. This results in a dilution effect. Additionally, the dye can bind to the tissue (solute-skin interaction), and, finally, there is some mixing with interstitial fluid, which probably can be neglected due to the total introduced volume ranging from 0.1 ml to 1.0 ml.

With PEG as a vehicle, the staining is not limited to the dermis and can also be found in the fatty hypodermis. This is due to the good solubility of PEG in polar and non-polar solvents. Capillary transport was also observed. However, the liquid escaping the skin sample was more stained compared to the case with water as vehicle. This is due to the fact that there are almost only capillaries that take up PEG from stained sites. Additionally, with PEG as vehicle, the affinity of gentian violet to bind to the tissue is reduced due to the good solubility in this vehicle. This is an indication for solute-vehicle interactions.

In our experiments we were not able to find any hint that the spot size would depend on skin samples of different pigs or different storage methods. Only the data of the skin of two out of 23 pigs showed statistically different results (ANOVA, $p<0.05$).

To finally achieve systemic drug delivery by intradermal administration it is necessary that the drug is taken up by the dermal capillaries. The efficiency of that route depends inter alia on the affected area within the highly capillarised dermal layer. Our results clearly show that the lateral distribution of gentian violet with PEG as vehicle covers approximately ten times larger areas compared to water-based solutions. Additionally, the gentian violet spreads into the hypodermis with PEG as vehicle.There are pros and cons of using PEG-based solutions. An advantage is the fact that by just using one individual cannula a quite large area

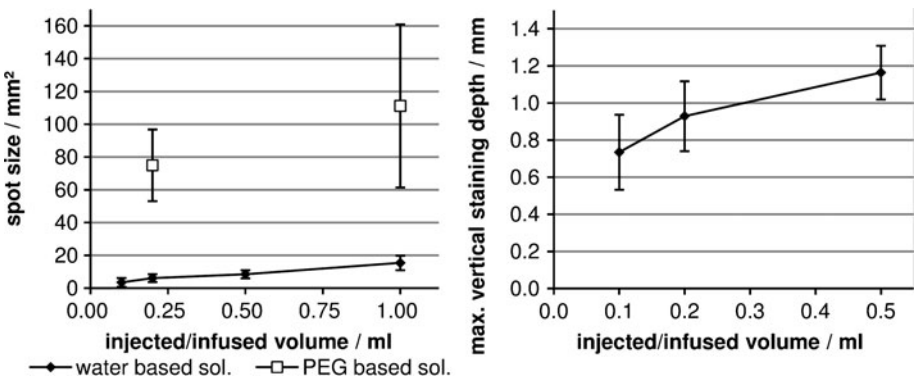

Fig. 9 Left: Spot size of intradermal infusions and injections into *ex vivo* pig skin, depending on delivered volume. Data of experiments with water- and PEG-based solution are given. Each data point represents 7–11 experiments. Right: The maximum vertical penetration depth of the staining in the tissue. Data of infusion/injection experiments with water-based solution and insertion parameters 4/2 is shown.

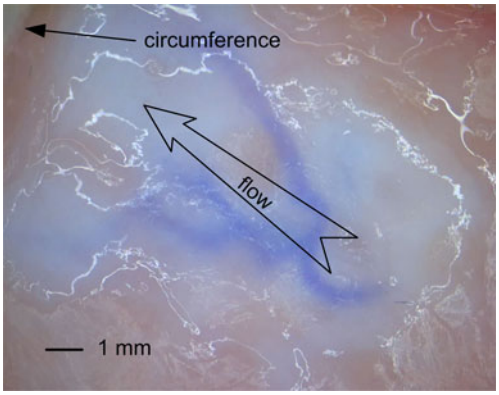

Fig. 10 Backside of a skin specimen after infusion of stained water with a flow rate of 0.10 ml/h and insertion parameter set 3/2. The capillaries turned blue and conducted liquid from the infusion site to the circumference of the skin specimen, indicated by the arrow.

within the dermis can be loaded with drug. In contrast, a potential risk in using PEG-based solutions is the fact that potentially some drug delivery to the bloodstream is delayed when the drug solution penetrates into the hypodermis and deeper tissues, as illustrated in Fig. 8, right. For water-based solutions, a single microneedle can stain a tissue area monitored from the top from 3.5 $mm^2 \pm$ 2.7 mm to 15 $mm^2 \pm 4.4$ mm^2, depending on the infused volume.

We showed that a solute can be separated form its vehicle during pressure-driven infusion/injection, for example, by binding of the solute to the tissue. Drug molecules probably show less tissue binding compared to a dye like gentian violet, so the affected skin area of such drugs by pressure-driven intradermal infusion/injection is supposed to be larger compared to the values given above.

Three major factors need to be considered in designing microneedle arrays. One major factor is the rate of absorption, which is supposed to be higher the larger the affected skin area is, so the higher the desired absorption rate, the more microneedles are necessary. Another major factor is the affected skin area by a single microneedle because it determines the density of microneedles in an array. We showed that this factor can be influenced by the injected volume and interactions of the vehicle with the skin, the solute and the skin, and the solute and the vehicle. The third major factor is the depth in the skin where the liquid containing the drug is infused/injected. With very small, hollow, leak-proof and short microneedles intra-epidermal infusions/injections would be possible.

A general limiting factor for intradermal infusions/injections is the solubility of the drug in the solution, hence, the total volume of delivered liquid. Injection volumes are probably limited to a volume of 0.20 ml, which is usually the maximum volume injected with the Mantoux method. It is supposed that larger volumes need to be infused at low infusion rates over longer periods of time so that the vehicle can be removed by the body. Of course, this is only possible if the duration of administration is not critical.

In the design of a microneedle interface one might end up with a solution based on a single microneedle. Continuous infusion of insulin might be such an application because insulin is currently infused via a single subcutaneous cannula.

Infusion/Injection Process

A transient back pressure was observed in the infusion/injection experiments. The back pressure signal of two infusion experiments with aqueous solution, a flow rate of 0.10 ml/h and insertion parameter sets 3/2 and 5/2 is presented in Fig. 11. The transient back pressure of the experiment with insertion parameters 3/2 shows an initial back pressure overshoot. The experiment with insertion parameters 5/2 shows almost no back pressure overshoot. Both signals finally reached a steady-state back pressure level for the rest of the experiment.

To get the steady-state back pressure level and information on the dynamics of the process the, data of the infusion experiments without back pressure overshoot were fit to the following equation:

$$p = p_A\left(1 - e^{-\frac{t}{\tau}}\right) \quad (1)$$

The time-dependent back pressure is denoted as p, the asymptotic steady-state back pressure as p_A, the time as t and the characteristic time constant as τ. The back pressure p reaches 63% of its asymptotic value within a time-span of τ and increases to 99% of the asymptotic value within five times of τ. The fit worked well for data without back pressure overshoot. The signals presented in

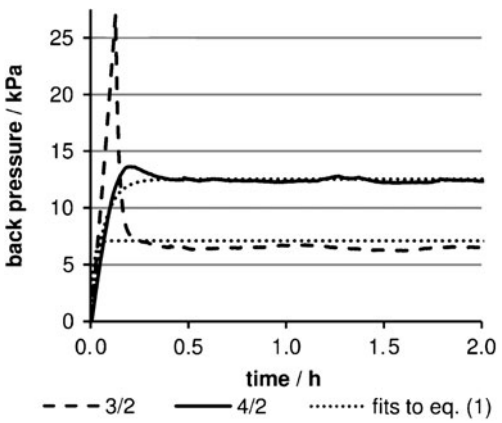

Fig. 11 Back pressure as a function of time for 2 intradermal infusion experiments with aqueous solution, a flow rate of 0.10 ml/h and insertion parameters 3/2 and 5/2. The *dotted lines* represent the fit of Eq. (1) to the data.

Fig. 11 resulted in coefficients of determination of 0.90 and 0.04 for experiments without and with back pressure overshoot, respectively. Table III gives an overview of the average coefficients of determination for infusion experiments without back pressure overshoot and identical parameters.

The series of experiments with a flow rate of 0.50 ml/h and insertion parameter set 4/2 showed a low coefficient of determination of 0.61. The main reason is a slight continuous decrease of −15%/h±4%/h (−4.9 kPa/h±1.3 kPa/h) of back pressure with time instead of a constant steady-state back pressure. The most probable reason is an undetected leak in the experimental setup. Two of the experiments with insertion parameter set 3/2 also showed this slight continuous decrease, which reduced the average coefficient of determination to 0.74. Experiments with coefficients of determination higher than 0.80 showed unstructured residuals.

If Eq. (1) is fit to data with back pressure overshoot, the parameter p_A is overestimated (Fig. 11). Therefore, in case of back pressure overshoot, the steady-state back pressure was determined by calculating the mean back pressure between 0.5 h and 2 h after start of the experiment.

The obtained steady-state back pressures give the total back pressures generated by the cannula and the tissue. Table IV gives an overview of total (measured) and cannula generated (see Materials and Methods section) back pressures at different flow rates and media.

The back pressure generated by the cannula is below 2% of the measured total value for infusion experiments with aqueous solution and flow rates ≤0.50 ml/h. However, in all other cases, the back pressure generated by the cannula accounts for 11%–19% of the measured values. Therefore, the back pressure generated by the cannula was subtracted from the total back pressure in order to plot the steady-state back pressure of the tissue as a function of flow rate in Fig. 12. The graph also shows data of the injection experiments. The back pressure generated by the experimental setup is neglected because the pressure sensor was mounted close to the cannula.

Table III Coefficients of Determination for Data of Infusion Experiments with Aqueous Solution Fit to Eq. (1). Experiments with Back Pressure Overshoot are Excluded.

Insertion parameter set	Flow rate	
	0.10 ml/h	0.50 ml/h
3/2	0.85 ± 0.01 (n = 2)	0.74 ± 0.13 (n = 6)
4/2	0.84 ± 0.13 (n = 7)	0.61 ± 0.13 (n = 8[a])
5/2	0.81 ± 0.13 (n = 7)	0.90 ± 0.06 (n = 7)

[a] One Experiment was omitted due to an exceptional constant increase (11 kPa/h) in back pressure. It could not be related to a full occlusion because stained liquid was infused into the skin and formed a spot with an area not distinguishable from other experiments with the same parameters.

At this stage, it is interesting to further characterise the tissue in terms of the back pressure that is needed to penetrate it with a defined liquid flow rate. The steady-state back pressure values of experiments with water-based solution (Fig. 12) can be fitted as $p \sim q^{0.53}$. It is consistent with previous work published in (11, Fig. 5). This data can be fitted as $p \sim q^{0.36\pm0.10}$. There is only a minor difference between the two exponents, which is most probably due to the fact that human cadaver skin instead of pig skin was used. The data clearly demonstrate that there is a nonlinear relationship between back pressure and flow rate. In other words, the fluidic resistance of the excised tissue is a function of flow rate. We further compared the back pressures needed for delivering PEG- and water-based solutions into the tissue. Although the viscosity of the two solutions differs by a factor of 55, the maximum pressure values only change roughly by a factor of 5 (factor 4.3 for 0.10 ml/h; factor 6.4 for 0.50 ml/h). This is a clear indication for vehicle-skin interactions.

The slightly higher exponent of the fitted back pressure data obtained with pig skin compared to the exponent of the fit to data from (11) obtained with human cadaver skin can be explained. Due to its higher density of collagen and other fibre bundles in the reticular dermis, pig skin shows an increased resistance to skin deformations (2), which are, for example, caused by the intradermal infusion/injection of liquid volume, so the back pressure of intradermal infusions/injections is higher in pig skin compared to human skin. Therefore, pig skin is a reasonable model to study the back pressure of intradermal infusions/injections if the focus is on obtaining an upper design limit.

The dynamics of infusion experiments without back pressure overshoot is described by the parameter τ of Eq. (1). An equivalent number was generated with the data with back pressure overshoot. In this case, it was obtained by reading the time when the signal reached 63% of the steady state value. The numbers were averaged together with τ and resulted in time constants of at least 2.3 min ± 1.2 min. (0.50 ml/h aqueous solution, n=27). The data of two experiments was excluded from the mean (11 min. and 14 min.) because of its strong influence on the mean, suggesting that there is a different unknown but rare mechanism at work. Further investigations revealed that the dynamics of the infusion process were mainly governed by the syringe pump.[2]

[2] According to the subsequent text the time constant of the experimental setup including the tissue can be calculated to be 0.7 min, with $R_{total,0.50\ ml/h}$ = 62 kPah/ml (calculated with data of Table IV) and C_{setup} = 0.2 μl/kPa (see subsequent text).

Table IV Total (Measured) and Cannula-Generated (See Materials and Methods Section) Back Pressures at Different Flow Rates with Media with Different Viscosities

	Back pressure / kPa					
	Aqueous solution				PEG solution	
	0.10 ml/h	0.50 ml/h	36 ml/h	180 ml/h	0.10 ml/h	0.50 ml/h
Total	11 ± 7	31 ± 18	261 ± 101	881 ± 76	47 ± 25	198 ± 149
Cannula	0.09	0.45	32	162	5	25

During the infusion experiments, the delivered liquid volumes were cross-checked with the integrated data of the flow sensor in the setup. Both values were within 10% deviation.

Back pressure overshoot was observed in 20 out of 56 infusion experiments with aqueous solution. Table V gives an overview of back pressure overshoots sorted by insertion parameter set and flow rate. The trend in the data suggests that the risk of an overshoot reduces with increasing tip depth and flow rate.

The duration of a back pressure overshoot was obtained by determining the time the signal exceeded the steady-state back pressure by 10%. These data are presented in Table VI together with the recorded average maximum back pressure. The recorded maximum values in a single experiment are 38 kPa (352% of steady-state back pressure) and 112 kPa (361% of steady-state back pressure) for flow rates of 0.10 ml/h and 0.50 ml/h, respectively.

Experiments performed with PEG solution showed no back pressure overshoot. This might be related with the aspect that, in general, higher pressure levels were needed in order to deliver PEG solutions at the same flow rate. Finally, we conclude that an initial back pressure overshoot can be present. This phenomenon is related to initial clogging of the cannula after its insertion. An initial back pressure overshoot of less than 400% of the steady-state back pressure was sufficient to remove the clogging.

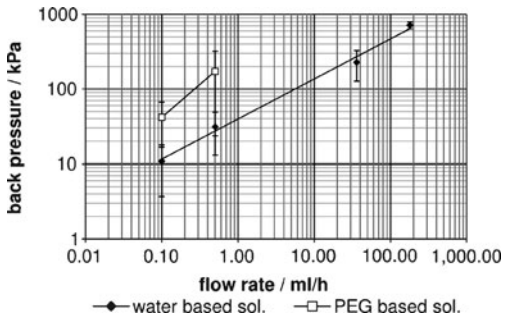

Fig. 12 Steady-state back pressures across the tissue for intradermal injections/infusions at different liquid delivery rates with water-based and PEG-based solutions. Delivery rates below 1 m/h belong to infusion experiments. Delivery rates above 1 ml/h belong to injection experiments. The *error bars* show the standard deviation (0.10 ml/h: $n=27$, aqueous sol.; 0.50 ml/h: $n=29$, aqueous sol.; all other data points $n=9$).

In manual injection experiments, only performed with water as vehicle, the back pressure followed a steep increase before it reached a constant steady-state level with superimposed irregular oscillations (Fig. 13). The nature of these oscillations was most likely due to the manual control of the injection procedure. The duration of the metronome-synchronised manual injection process is 9.3 s ± 0.4 s ($n=18$). It was measured from the beginning of the steep increase to the beginning of the decay.

To extract the values of the constant steady-state back pressure level, the back pressure values within the band of oscillations were averaged. This band is defined by the maximum back pressure and the minimum back pressure between the steep increase and final decrease of the signal (Fig. 13). To derive quantitative results, we extracted the characteristic time t_1 for which 90% of the constant back pressure level was reached. t1 is determined as 5.7 s ± 2.3 s. Further analysis is disputable because it is mixed with the manual injection process.

The back pressure decay fits very well to an exponential behaviour described by

$$p = p_0 + p_D e^{-\frac{t}{\tau}} \quad (2)$$

The time-dependent back pressure is denoted as p, the residual back pressure at the end of the decay with p_0, the back pressure at the beginning of the decay is the sum of p_D and p_0, and the time constant is denoted with τ. The coefficient of determination is 0.97 ± 0.02 ($n=18$). The average residual pressure p_0 is less than 1% of the average constant steady-state back pressure level. The time constants of the back pressure decays are 5.1 ± 1.8 s ($n=9$) and

Table V Summary of Back Pressure Overshoots in Infusion Experiments with Aqueous Solution. Every Flow Rate and Insertion Parameter Set Combination was Realised 9 Times.

Insertion parameter set	Flow rate	
	0.10 ml/h	0.50 ml/h
3/1	7	4
4/2	2	2
5/3	3	2

Table VI Duration and Average Maximum Back Pressure of Back Pressure Overshoots with Aqueous Solution at Flow Rates 0.10 ml/h and 0.50 ml/h

Flow rate / ml/h	Cases	Duration / min.	Average max. / kPa
0.10	12	20 ± 9	18 ± 9
0.50	8	15 ± 9	40 ± 33[a]

[a] Excluding one experiment, with an exceptional back pressure overshoot of 112 kPa, the average absolute max. is 30 kPa ± 16 kPa

3.1 ± 0.9 s (n=9) for injection flow rates of 36 ml/h and 180 ml/h, respectively. The ratio of the time constants is 1.6.

The high coefficient of determination is a strong indication that changes in τ during back pressure decay of a single experiment can be neglected. Taking this as a basis, the time constant can be calculated according to the model assumption (see Materials and Methods section) to

$$\tau_q = (R_{cannula} + R_{tissue}) \cdot C_{setup} \quad (3)$$

The time constant affiliated with the flow rate q is denoted as τ_q, the fluidic resistivity of the cannula as $R_{cannula}$, the fluidic resistivity at flow rate q of the tissue as $R_{tissue,q}$ and the fluidic capacity of the setup as C_{setup}. With R_{tissue} as a function of flow rate and assuming C_{setup} is constant, one can calculate the ratio of time constants according to

$$\frac{\tau_{low}}{\tau_{high}} = \frac{R_{cannula} + R_{tissue,low}}{R_{cannula} + R_{tissue,high}} \quad (4)$$

The subscripts low and high denote the corresponding time constant τ and fluidic resistivity R in the case of injection experiments with low (36 ml/h) flow rate and high (180 ml/h) flow rate. With $R_{tissue,low}$ of 6.3 kPa h/ml, $R_{tissue,high}$ of 4.0 kPa h/ml (both values calculated with data of Table IV) and $R_{cannula}$ of 0.9 kPa h/ml (see Materials and Methods section) the ratio of the time constants is 1.5. This is just a minor deviation form the ratio of the measured time constants, so the structure of the assumed model is acknowledged with a flow rate-dependent tissue resistivity.

The fluidic capacity of the experimental setup can be calculated by solving Eq. (3). The measured fluidic resistivities and measured time constants of intradermal injection experiments with water resulted in a fluidic capacity of 0.19 µl/kPa. The data of experiments without skin (τ=0.50 s ± 0.04 s, q=180 ml/h, n=3) results in a fluidic capacity of 0.15 µl/kPa, which is close to the value obtained from the measured data. The fluidic capacity of the experimental setup is quite high. A simple syringe with cannula is supposed to exhibit a much lower capacity.

The high back pressures observed in the injection experiments demands as a good practice leaving the cannula inserted into the skin for a multiple of time constants when the injection is finished. Otherwise, a small droplet of liquid appears on the skin surface, which might result in inconsistent drug delivery. The time constants observed in this work are quite long due to the high capacity of the experimental setup. A simple syringe cannula combination with a substantial lower capacity will result in shorter time constants.

For infusion experiments and injection experiments, we saw no hint that the asymptotic back pressure levels or the time constants would depend on skin samples from different pigs or different storage conditions.

The phenomena of varying flow resistance of the tissue and the overshoot in back pressure might influence the proper selection of drug delivery actuation mechanisms for intradermal drug delivery devices.

The data presented so far were obtained in *ex vivo* experiments with excised tissue. It is assumed that the infusion at low flow rates (0.1 ml/h) and injection of small volumes (0.1 ml) *in vivo* results in steady-state back pressures comparable to the presented values because an infusion/injection volume of 0.10 ml is less than 10% of the average volume (1.77 ml ± 0.32 ml) of the skin specimens. This assumption needs to be checked in *in vivo* experiments.

The limiting issue for intradermal infusions is the initial back pressure overshoot, which is almost 400% higher compared to the steady-state back pressure. At this stage, there is no reason to believe that the data of the initial back pressure overshoot obtained in the *ex vivo* experiments is not valid in the *in vivo* case, so, for reliable infusions, a suitable device must be able to generate pressures from 38 kPa to 112 kPa for infusion flow rates of 0.10 ml/h to 0.50 ml/h, respectively. This is not self-evident for a micro actuator (20,23). Currently, small skin attachable programmable or intelligent infusion devices based on micro actuators seem to be feasible if a flow rate of approximately 0.10 ml/h is sufficient for the application. Substantial higher flow rates

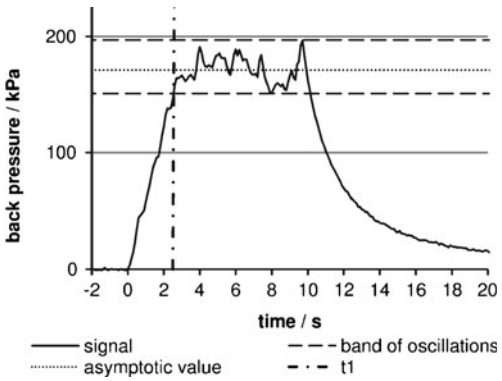

Fig. 13 Back pressure as a function of time for a manual intradermal injection of 0.10 ml of aqueous solution with insertion parameter set 4/2. The asymptotic value was determined by averaging the data within the band of oscillations. t1 is the time when the signal reached 90% of the asymptotic value.

resulting in higher back pressures in the order of more than 100 kPa definitely require more powerful drive systems for intelligent infusion systems, e.g. electromechanical drives.

Relevance of the Technology

The laboratory setup was designed in order to study the influence of different penetration parameters. For the sake of convenience in performing these experiments, its size was set for easy handling. Therefore, it is quite large. If the penetration parameters are fixed, its size can be shrunk to a minimum. However, even with estimated dimensions of 14 mm×12 mm×10 mm (corresponding to a volume of 1.7 ml), the shrunk intradermal interface will be much bulkier compared to out-of-plane microneedle designs. This is not necessarily a drawback. The intradermal interface is best utilised in intelligent infusion devices which are worn for longer periods of time. Hence, the device also needs to store a supply of drug solution, a drive mechanism, electronics, battery and a user interface. This functionality may be realised by insulin pumps. The current smallest one on the market (Omnipod by Insulet, Bedford, MA, USA) has a size of 45 ml. Therefore, the presented mechanism shrunk to the estimated size is considered an alternative interface to the human for intelligent infusion devices.

The presented intradermal interface in combination with a suitable delivery device can infuse liquids in continuous or intermittent fashion. It is conceivable to control the intermittent infusion, for example, in response to a sensor input. Of course, it can also be used to inject liquids into the skin. The infused/injected liquids can be solutions of hydrophilic, ionic and macromolecular drugs. However, the rate of uptake of these molecules from the tissue into the systemic circulation needs to be studied.

CONCLUSIONS

We presented an intradermal interface which enables placing a cannula into the dermis by simply pushing and releasing a slider. It is minimally invasive and allows infusing or injecting liquids containing hydrophilic, ionic and macromolecular drugs into the dermis. This mechanism could be an important building block of complete drug delivery systems for time-, user- or sensor-controlled drug delivery. The cannula insertion mechanism is so simple that it could be applied for self-administration of drugs.

We investigated three different failure modes for leakage and proofed that the intradermal interface showed excellent leak tightness. Although a leakage occurred in nine out of 92 experiments, this leakage never happened at the puncture site. We expect to be able to exclude a first leakage failure mode by properly selecting an application site with low hair follicle density. In a second and third leakage failure mode, we were only able to detect a small leakage of clear carrier fluid without staining, so it is very likely that no drug molecules are lost by those leakage failure modes. This needs to be checked in *in vivo* experiments preferably in humans.

The volume of the stained tissue can depend on vehicle-skin, vehicle-solute and solute-skin interactions. With water as vehicle, the distribution of the model drug (gentian violet) and the vehicle were limited to the dermal layer involving solute-skin and vehicle-skin interactions. The maximum vertical staining depth was 1.16 mm± 0.14 mm. The lateral penetration depth resulted in stained areas of 3.5 $mm^2 \pm 2.7$ mm^2 to 15 $mm^2 \pm 4.4$ mm^2 monitored from the top. With PEG as vehicle, the stained tissue area is almost one order of magnitude larger compared to the water-based solution involving vehicle-solute interactions. In this case, penetration of stained PEG into the hypodermis was observed. If a given tissue area should be loaded with drug, these interactions need to be considered. For water-based solutions, the presented data can be regarded as lower limit because drug molecules show probably less tissue binding compared to the dye gentian violet.

The infusion/injection process initiated with a flow source showed occasional initial back pressure overshoot. Values ranging from 38 kPa to 112 kPa for flow rates from 0.10 ml/h to 0.50 ml/h were measured. This back pressure overshoot was identified as the limiting parameter for the design of small programmable or intelligent devices based on micro actuators.

The *ex vivo* experiments revealed a flow rate-dependent tissue back pressure. The back pressure needed for infusing PEG-based solutions was only about a factor of five higher compared to the back pressure needed to infuse water, although the viscosities vary roughly by a factor of 55. This is due to solute-skin interactions. In general, we found that steady-state back pressures in the order of 11 kPa ± 7 kPa to 198 kPa ± 149 kPa are needed for the infusion of water- and PEG-based solutions at flow rates of 0.10 ml/h and 0.50 ml/h, respectively. *In vivo* back pressures might be higher and need to be studied.

With the presented intradermal interface, it is possible to deliver liquids reliably to the intradermal layer of the skin. A large variety of drugs dissolved in this liquid can be infused with high temporal and quantitative precision compared to oral drug administration if the intradermal interface is combined with a suitable skin attachable drug delivery actuation mechanism. Consequently, the authors are convinced that the smart intradermal interface has the potential to be a clinically relevant building block for easy-to-use self administration of drugs.

ACKNOWLEDGMENTS

We gratefully acknowledge financial support from the Landesstiftung Baden-Württemberg (contract number 4-4332.62-HSG/34). We are also highly thankful to Dr. Barke for providing us with pig skin.

REFERENCES

1. Holland D, Booy R, De Looze F, Eizenberg P, McDonald J, Karrasch J, *et al.* Intradermal influenza vaccine administered using a new microinjection system produces superior immunogenicity in elderly adults: a randomized controlled trial. J Infect Dis. 2008;198:650–8.
2. Laurent PE, Bonnet S, Alchas P, Regolini P, Mikszta JA, Pettis R, *et al.* Evaluation of the clinical performance of a new intradermal vaccine administration technique and associated delivery system. Vaccine. 2007;25:8833–42.
3. Van Damme P, Oosterhuis-Kafeja F, Van der Wielen M, Almagor Y, Sharon O, Levin Y. Safety and efficacy of a novel microneedle device for dose sparing intradermal influenza vaccination in healthy adults. Vaccine. 2009;27:454–9.
4. Gupta J, Felner EI, Prausnitz MR. Minimally invasive insulin delivery in subjects with type 1 diabetes using hollow microneedles. Diabetes Technol Ther. 2009;11:329–37.
5. Cross S, Roberts M. Physical enhancement of transdermal drug application: is delivery technology keeping up with pharmaceutical development? Curr Drug Deliv. 2004;1:81–92.
6. Prausnitz MR, Langer R. Transdermal drug delivery. Nat Biotechnol. 2008;26:1261–8.
7. Banga AK. Microporation applications for enhancing drug delivery. Expert Opin Drug Deliv. 2009;6:343–54.
8. Gardeniers HJGE, Luttge R, Berenschot EJW, de Boer MJ, Yeshurun SY, Hefetz M, *et al.* Silicon micromachined hollow microneedles for transdermal liquid transport. J Microelectromech Syst. 2003;12:855–62.
9. Griss P, Stemme G. Side-opened out-of-plane microneedles for microfluidic transdermal liquid transfer. J Microelectromech Syst. 2003;12:296–301.
10. Stoeber B, Liepmann D. Arrays of hollow out-of-plane microneedles for drug delivery. J Microelectromech Syst. 2005;14:472–9.
11. Martanto W, Moore JS, Kashlan O, Kamath R, Wang PM, O'Neal JM, *et al.* Microinfusion using hollow microneedles. Pharm Res. 2006;23:104–13.
12. Khumpuang S, Horade M, Fujioka K, Sugiyama S. Geometrical strengthening and tip-sharpening of a microneedle array fabricated by X-ray lithography. Microsyst Technol. 2007;13:209–14.
13. Bodhale D, Nisar A, Afzulpurkar N. Structural and microfluidic analysis of hollow side-open polymeric microneedles for transdermal drug delivery applications. Microfluid_Nanofluid. 2010;8:373–92.
14. Kim K, Park DS, Lu HM, Che W, Kim K, Lee JB, *et al.* A tapered hollow metallic microneedle array using backside exposure of SU-8. J Micromech Microeng. 2004;14:597–603.
15. Verbaan FJ, Bal SM, van den Berg DJ, Dijksman JA, van Hecke M, Verpoorten H, *et al.* Improved peircing of microneedle arrays in dermatomed human skin by an impact insertion method. J Control Release. 2008;128:80–8.
16. Verbaan FJ, Bal SM, van den Berg DJ, Groenink WHH, Verpoorten H, Lüttge R, *et al.* Assembled microneedle arrays enhance the transport of compounds varying over a large range of molecular weight across human dermatomed skin. J Control Release. 2007;117:238–45.
17. Heinemann L, Pettis RJ, Hirsch LJ, Nosek L, Kapitza C, Sutter DE, *et al.* Microneedle-based intradermal injection of lispro or human regular insulin accelerates insulin uptake and reduces postprandial glycaemia. Diabetologia. 2009;52:963.
18. Donnelly RF, Singh TRR, Tunney MM, Morrow DIJ, McCarron PA, O'Mahony C, *et al.* Microneedle arrays allow lower microbial penetration than hypodermic needles *in vitro*. Pharm Res. 2009;26:2513–22.
19. Häfeli UO, Mokhtari A, Liepmann D, Stoeber B. *In vivo* evaluation of a microneedle-based miniature syringe for intradermal drug delivery. Biomed Microdevices. 2009;11:943–50.
20. Nisar A, AftuIpurkar N, Mahaisavariya B, Tuantranont A. MEMS-based micropumps in drug delivery and biomedical applications. Sens Actuat B Chem. 2008;130:917–42.
21. Matteucci M, Casella M, Bedoni M, Donetti E, Fanetti M, De Angelis F, *et al.* A compact and disposable transdermal drug delivery system. Microelectron Eng. 2008;85:1066–73.
22. Lemmer B. Chronobiology, drug-delivery, and chronotherapeutics. Adv Drug Deliv Rev. 2007;59:825–7.
23. Iverson BD, Garimella SV. Recent advances in microscale pumping technologies: a review and evaluation. Microfluid Nanofluid. 2008;5:145–74.
24. Henning A, Neumann D, Kostka KH, Lehr CM, Schaefer UF. Influence of human skin specimens consisting of different skin layers on the result of *in vitro* permeation experiments. Skin Pharmacol Physiol. 2008;21:81–8.
25. Sepassi K, Yalkowsky SH. Solubility prediction in octanol: a technical note. AAPS PharmSciTech. 2006;7:E26.
26. Yamaoka T, Tabata Y, Ikada Y. Distribution and tissue uptake of poly(ethylene glycol) with different molecular weights after intravenous adminsitration to mice. J Pharm Sci-US. 1994;83:601–8.
27. Santhanalaksmi J, Balaji S. Binding studies of crytsal violet on proteins. Colloids Surf A. 2001;186:173–7.
28. Bonnekoh B, Wevers A, Jugert F, Merk H, Mahrle G. Colorimetric growth assy for epidermal cell cultures by their crystal violet binding capacity. Arch Dermatol Res. 1989;281:487–790.
29. Saji M, Taguchi S, Uchiyama K, Osono E, Hayama N, Ohkuni H. Efficacy of gentian violet in the eradication of methicillin-resistant staphylococcus aureus from skin lesions. J Hosp Infect. 1995;31:225–8.